Purification strategies and purity visualization techniques for single-walled carbon nanotubes

Tae-Jin Park,[a] Sarbajit Banerjee,[a] Tirandai Hemraj-Benny[a] and Stanislaus S. Wong*[ab]

Received 12th April 2005, Accepted 2nd August 2005
First published as an Advance Article on the web 30th August 2005
DOI: 10.1039/b510858f

Traditionally, SWNTs have been prepared by electric arc-discharge, laser ablation, or chemical vapor deposition (CVD) methods, yielding tubes of various diameter and length distributions. However, without exception, as-prepared SWNTs are contaminated with a number of impurities, decreasing the overall yield of usable material. Impurities include transition metal catalysts, such as Fe, Co, and Ni, which are necessary for the growth of SWNTs as well as carbonaceous species such as amorphous carbon, fullerenes, multishell carbon nanocapsules, and nanocrystalline graphite. In this Feature Article, we highlight the role of microscopy in designing and facilitating the interpretation of the success of strategies, including (a) oxidative methods including liquid and gas phase oxidation, (b) chemical functionalization protocols, (c) filtration and chromatography techniques, and (d) microwave heating methods, aimed at rationally purifying single-walled carbon nanotubes.

1. Introduction

Since the discovery of single-walled carbon nanotubes (SWNTs),[1] there have been a large number of investigations of these materials, due to their unique one-dimensional structure and their exceptional structure-dependent properties.[2] Because of their seamless cylindrical graphitic shells, carbon nanotubes might be stiffer and stronger than potentially any other known material with implications for the design of composite materials as well as nanometre-scale devices. Not only do these tubes possess extremely desirable mechanical properties of strength and flexibility, but also their electronic properties range from metallic to semiconducting depending on their structure. It is not surprising therefore that SWNTs have been considered as excellent candidates for many potential applications, including, but not limited to: catalyst supports in heterogeneous catalysis,[3] high-strength composites,[4] sensors,[5,6] actuators,[7] gas storage media,[8–10] field emitters,[11,12] tips for scanning probe microscopy,[13] and nanoelectronic devices.[14–18] However, in order for the vast potential of these materials to be fulfilled and moreover, in order to investigate the fundamental physical and chemical properties of SWNTs, extensive purification protocols are required to obtain reproducibly reliable material.

SWNTs have been prepared by electric arc-discharge,[19] laser ablation,[20,21] or chemical vapor deposition (CVD)[22] methods, yielding tubes of various diameter and length distributions. However, as-prepared SWNTs are typically contaminated with

[a]*Department of Chemistry, State University of New York at Stony Brook, Stony Brook, NY, 11794-3400, USA. E-mail: sswong@notes.cc.sunysb.edu, sswong@bnl.gov; Tel: +1 631 632 1703, +1 631 344 3178.*
[b]*Materials and Chemical Sciences Department, Brookhaven National Laboratory, Building 480, Upton, NY, 11973, USA*

Tae-Jin Park

Tae-Jin Park was born in Seoul, Korea. He earned BSc and MSc degrees in Chemistry from Yonsei University in 1997 and 1999, respectively. After completing compulsory military service in 2001, he worked as a research scientist at the Korea Institute Science Technology (KIST). He is currently pursuing a PhD degree in the Department of Chemistry at the State University of New York under the supervision of Prof. Stanislaus S. Wong. His research interests include the structural characterization of carbon nanotubes as well as the synthesis and characterization of nanoscale functional materials, such as metal oxide perovskites.

Sarbajit Banerjee

Sarbajit Banerjee was born in Calcutta, India in 1978. From 1997 to 2000, he was a Sumitomo Corporation Scholar at St Stephen's College, University of Delhi where he obtained a BSc (Honors) degree in Chemistry. He completed his PhD in Chemistry at the State University of New York at Stony Brook in August 2004 under the direction of Prof. Stanislaus S. Wong. His thesis focused on the surface chemistry and differential reactivity of carbon nanotubes and the study of modified nanotubes using vibrational spectroscopies and X-ray absorption spectroscopy. Currently, he is a postdoctoral research scientist with Prof. Irving P. Herman at the Center for Nanoscale Science and Engineering at Columbia University.

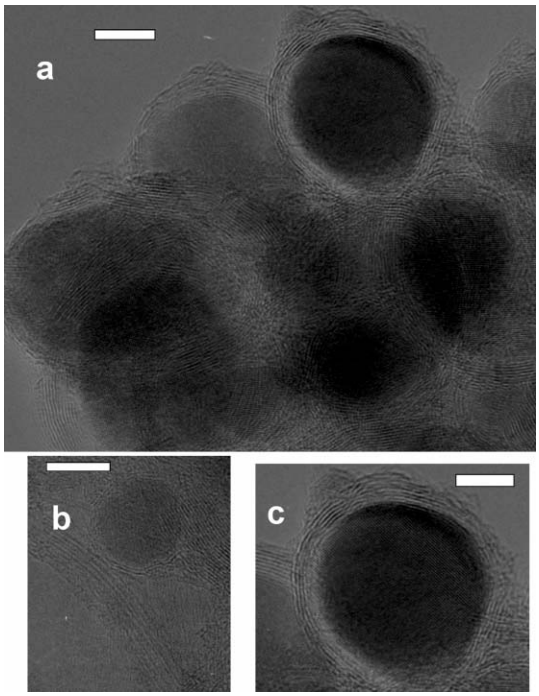

Fig. 1 (a) Cluster of iron particles, embedded in graphitic shells, in a HiPco SWNT sample. (b) SWNT ropes, along with a contaminant iron particle. (c) Lattice-resolved image of a graphite-encapsulated iron particle in a HiPco sample. The scale bars indicate 3.5 nm, 7.5 nm, and 3.0 nm, respectively.

a number of impurities, decreasing the overall yield of usable material.[23] Impurities include transition metal catalysts, such as Fe, Co, and Ni, which are necessary for the growth of SWNTs (Fig. 1). Carbonaceous species such as amorphous carbon, fullerenes, multishell carbon nanocapsules, and nanocrystalline graphite, are also problematic (Fig. 2). These contaminants can potentially show up in ensemble measurements

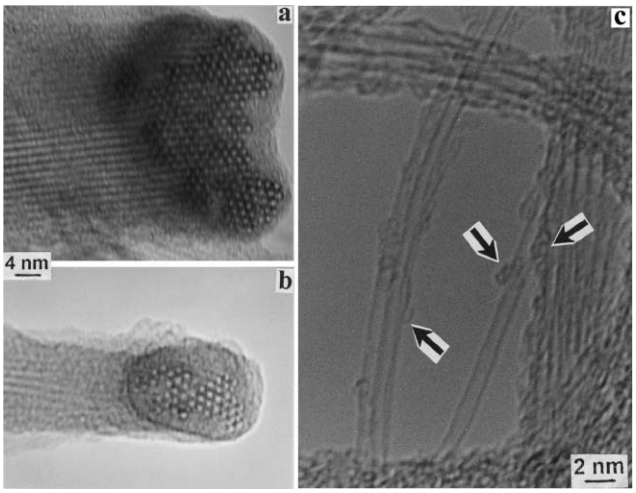

Fig. 2 (a) and (b). Two examples of SWNT rope 'cross-sections' (*i.e.* the projections of bent ropes whose bent part is oriented parallel to the electron beam) for as-prepared SWNT material produced from PLV. Ropes are evidently coated with amorphous material. (c) The occurrence of fullerene molecules (arrows) on the SWNT surface is shown when isolated SWNTs (as-prepared material from PLV) are imaged. Reprinted with permission from ref. 48, M. Monthioux, B. W. Smith, B. Burteaux, A. Claye, J. E. Fischer, D. E. Luzzi, *Carbon*, 2001, **39**, 1251. Copyright (2001) Elsevier.

using a number of different analytical techniques including Raman spectroscopy, UV–visible–NIR spectroscopy, fluorescence emission spectroscopy, X-ray photoelectron spectroscopy (XPS), near-edge X-ray absorption fine structure spectroscopy (NEXAFS), nuclear magnetic resonance (NMR) spectroscopy and X-ray diffraction.

An important area of carbon nanotube research in our research group has focused on developing rational chemical functionalization strategies for these materials.[23a] Performing chemistry with SWNTs, though, requires a ready supply of

Tirandai Hemraj-Benny

Tirandai Hemraj-Benny was born and raised in Georgetown, Guyana. She completed her BSc in chemistry at The City University of New York, York College in 2001. Since then, she has been working on her doctoral thesis, based on studies of carbon nanotubes, at the State University of New York at Stony Brook under the supervision of Prof. Stanislaus S. Wong. Her research interests include the rational chemical functionalization and purification of carbon nanotubes and the development of novel physical characterization protocols of these materials.

Stanislaus S. Wong

Stanislaus S. Wong earned a BSc (First Class Honours) from McGill University in 1994 and subsequently completed his PhD thesis from Harvard University in 1999 under the tutelage of Prof. Charles M. Lieber. After finishing a postdoctoral fellowship at Columbia University with Prof. Louis E. Brus, he has held the position, since September 2000, of Assistant Professor in Chemistry at the State University of New York (SUNY) at Stony Brook with a joint appointment at Brookhaven National Laboratory. He and his group have wide-ranging interests in nanotechnology, including the rational chemical functionalization of carbon nanotubes, the synthesis and characterization of metal oxide nanostructures (such as perovskites), the development of synchrotron-based techniques for nanoscale characterization, and the use of probe microscopy to initiate localized chemistry. Prof. Wong has been a 3M non-tenured faculty fellow since 2002 and earned a National Science Foundation CAREER award in 2003.

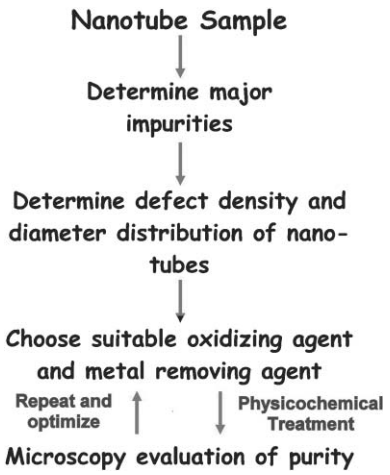

Fig. 3 Schematic depiction of a viable SWNT purification protocol.

relatively pure SWNT samples. In addition, it is evident that the presence of contaminants renders it difficult to understand and to monitor the intrinsic properties of SWNTs. Moreover, contamination interferes with the unequivocal interpretation of data obtained from various characterization protocols. For example, iron fluorescence under Cu Kα radiation makes it effectively impossible to study bundling in HiPco SWNTs by XRD using a conventional laboratory diffractometer.[24] In many laboratories, particularly ours, the algorithm for the rational purification of nanotubes involves (i) determination of major existing impurities, (ii) analysis of approximate diameter distributions and defect densities in samples, (iii) choice of appropriate oxidizing and metal leaching agents, (iv) microscopic evaluation of sample purity, and (v) iteration and optimization of steps (iii) and (iv). This general methodology for sample purity evaluation is depicted in Fig. 3.

As mentioned, the first step involves the determination of impurities and is commonly performed using electron microscopy (EM). Understanding the nature of impurities that need to be targeted by further chemical treatment is critical to the design of rational purification strategies. Whereas metal catalysts and fullerenes are relatively easy to remove, amorphous carbon and graphitic carbon are more difficult to eliminate because they have a similar oxidation temperature as that of SWNTs. In addition, the presence of graphitic carbon-encapsulated metal catalysts is a fundamental challenge to nanotube purification as metal removal tends to be invariably coupled with a high degree of tube destruction.

An estimate of the defect density and diameter distribution of nanotubes is important in choosing the correct oxidizing agent. Specifically, this means that aggressive oxidation reagents cannot be used with tubes, which have a high density of defects, *e.g.*, CVD grown tubes. In general, the reactivity of nanotubes is correlated with diameter. Smaller diameter nanotubes are more strained and thus show a greater reactivity towards addition reactions that relieve strain. Moreover, tubes fabricated by the high pressure decomposition of CO (HiPco) process, which have relatively smaller diameters in the range of 0.7–1.1 nm as compared with conventional types of tubes made by other methods (usually 1.4 nm), can be almost completely destroyed by aggressive oxidation and purification methods. Thus, different purification protocols are required for SWNTs grown from different synthetic processes. Recent advances in nanotube science[23c] focus on separating nanotubes by chirality and diameter. In this Feature Article, however, we focus on the removal of extraneous impurities and contaminants from nanotubes.

1.1. Analytical techniques for the evaluation of SWNT purity

To evaluate the purity of SWNTs, a number of different analytical techniques, including Raman spectroscopy, UV–vis–NIR spectroscopy, thermogravimetric analysis (TGA), and microscopy, have been used. Each technique has its own advantages and disadvantages for purity evaluation, and each is complementary to the others.

Raman spectroscopy allows for an ensemble measurement for an entire sample. Raman spectra of SWNTs show three important regions: (a) the radial breathing mode (RBM) which is dependent on the diameter of the tube, (b) the tangential mode, also known as the G band, in the 1515 to 1590 cm^{-1} region, and (c) the disorder mode D band in the 1280–1320 cm^{-1} region. While the tangential mode (the G band) shows distinctive behavior modes for metallic and semiconducting nanotubes, the disorder mode (the D band) arises from a number of different origins: amorphous carbon, defects, poor graphitization, as well as functionalized (and thus sp^3-hybridized) carbons. Graphitic nanoparticles, of course, are far more defective than the well-crystallized nanotubes, and thus contribute much more to the D band intensity. Thus the D to G band intensity (I_D/I_G) ratio provide us with an estimation of sample purity. An increase in the relative intensity of the G band is consistent with an improvement in the proportion of usable SWNTs, and the decreased I_D/I_G ratio arises from a decreased quantity of carbonaceous species.[25] However, the Raman spectra cannot provide direct information on the nature of metal impurities. In addition, Raman spectroscopy is not a very useful tool for studying samples with low contents of amorphous carbon, *e.g.*, HiPco nanotubes.

UV–vis–Near IR spectroscopy has recently been reported as an important tool for quantitatively estimating the purity of a bulk nanotube sample.[26–28] Current synthetic techniques produce SWNTs with a range of chiralities and diameters, leading to a mixture of metallic and semiconducting SWNTs in samples produced. Since SWNTs give rise to a series of predictable electronic band transitions between van Hove singularities in the density of state (DOS) of nanotubes (S_{11}, S_{22}, and M_{11}), these interband transitions produce prominent features, which can be used to analyze the SWNT type and diameter distribution. Specifically, Haddon *et al.* have proposed a quantitative criterion for purity based on the integrated intensity of the S_{22} transitions as compared with the S_{22} intensity of a reference sample. However, the reproducible preparation of standardized SWNT films is difficult, and control of film thickness is not a trivial task. Moreover, this method relies solely on measuring semiconducting nanotubes. As different synthetic methods yield different distributions of metallic and semiconducting tubes,[29] it is hence difficult to compare purity levels across a wide range of different samples.

Thermogravimetric analysis (TGA) is useful in accurately estimating the amount of metal catalyst particles remaining in the sample.[30–32] When heated in air, impure tubes burn at lower temperatures, due to the presence of metal particles. One of the problems of this measurement is the need for sample destruction; it needs to be totally burnt in order for an accurate assessment of purity to be made. In addition, this bulk technique cannot easily distinguish between various forms of carbonaceous species such as amorphous carbon, graphitic carbon, and fullerenes.

Microscopy techniques allow for careful investigation of bundles or individual SWNT samples. Thus, techniques such as transmission electron microscopy (TEM), scanning electron microscopy (SEM), and atomic force microscopy (AFM) provide an excellent local structure probe for monitoring the purification process. They are qualitatively very useful and iterative techniques for the visualization of major impurities, the estimation of defect site density, and the analysis of the diameter distributions of NT materials. One of the limitations of microscopy, though, is that it can only be performed on a small, localized fraction of the sample.

Although several examples for quantitative analysis by electron microscopy (EM) exist,[33–35] it is unlikely that microscopy can be reliably or routinely used for quantification of sample purity. In effect, to quantitatively evaluate the purity of the samples, the volume fraction of each carbon species has to be estimated by averaging over a number of sample images, which may or may not be representative of the entire sample, as the process may be somewhat subjective.[36]

1.2. Purity from a chemical functionalization perspective

In our laboratory, we are focused on generating rational chemical strategies for functionalization of carbon nanotubes. Our previous work has centered on the role of carbon nanotubes as chemical ligands with distinctive sites for molecular modification,[37–41] and we have demonstrated the use of these functionalized nanotubes for applications such as catalysis support media.[42] In general, we have been very interested in nanotube functionalization with organic moieties and with nanocrystals as well as with inorganic molecular complexes as a means of enhancing and understanding nanotube solubilization, charge transfer, separation by diameter and chirality, as well as processability.[43–45] Hence, we are very involved with developing rational nanotube purification techniques utilizing the differential reactivity of nanotubes, as compared with other forms of carbon, to ensure the reliability and reproducibility of our chemical functionalization strategies. In discussions of our efforts as well as those of other groups in this regard, we focus primarily on the use of microscopy to evaluate the extent of the purity of nanotube samples, since microscopy allows for the accurate identification of SWNT structures and major associated impurities.

2. SWNT purification methods

In this Feature, we analyze a number of different purification strategies. These are classified as (a) oxidative methods including liquid and gas phase oxidations, (b) chemical functionalization protocols, (c) filtration and chromatography techniques, and (d) microwave heating methods. We will focus a lot of the discussion on oxidative methods, since they have the potential to be scaled up for use in treating and processing large quantities of SWNT materials.

As mentioned previously, as-prepared SWNTs contain two types of impurities: transition metal catalyst particles (typically Fe, Co, and Ni), and carbonaceous species, including amorphous carbon, fullerenes, multishell carbon nanocapsules, and nanocrystalline graphites. Representative micrographs for impurities, which could be generated from synthetic processes, are shown in Figs. 1 and 2. Fig. 1 shows TEM images of metal catalysts as well as multishell carbon nanocapsules, *i.e.* graphitic spheres encapsulating the iron particles. These are the major impurities in HiPco samples. As-prepared SWNTs from other synthetic processes also have similar types of metal impurities (usually Fe, Co, and Ni). Figs. 2a and 2b show examples of SWNT rope cross-sections coated with amorphous carbon, and Fig. 2b shows the presence of fullerene molecules, as indicated by arrows, coating the SWNTs surface. Thus, purification protocols have been primarily focused on eliminating the above-mentioned impurities during the chemical treatment processes without physically destroying either structural tube integrity or intrinsic (*i.e.*, electronic) properties. Microscopy evaluation of as-prepared SWNT samples thus helps in identifying the major impurities.

Herein, while not an exhaustive list by any means, we describe a selection of the most common purification strategies of SWNTs. We will primarily focus on the use of microscopy towards designing purification protocols and in evaluating the purity of SWNT samples.

2.1. SWNT purification methods based on oxidation

Oxidative methods have often been employed for nanotube purification due to their practicality, relative simplicity, applicability to both metal catalysts and amorphous carbons, prior versatility in chemical processes, and capability of purifying large quantities of nanotubes. Moreover, these techniques can often introduce oxygenated functional groups, such as carboxylic acids, which serve as a good starting point for subsequent nanotube surface chemistry.[46,47] These treatments include liquid phase oxidation treatment, such as acid treatment (HNO_3, HCl, $KMnO_4/H_2SO_4$, *etc.*) and/or refluxing in water or H_2O_2, as well as gaseous phase oxidation (using O_2, H_2 or air). It is believed that oxidants breach the carbon shell and then oxidize the metal catalysts to the corresponding metal oxide or hydroxide.[32] When the metal is oxidized, the volume increases and the metal oxides crack open the carbon coatings. Furthermore, oxidants tend to initially attack SWNTs from the ends, which have the more highly strained five-membered rings. However, amorphous carbon can be attacked from all sides leading to its preferential removal over SWNTs. All of these oxidation processes, which are accompanied by dissolution and leaching out of the metal/metal oxide impurities (often necessitating a separate procedure to remove the metal itself), generally yield relatively pure SWNTs.

The main disadvantage of oxidative treatments is that they tend to destroy not only impurities but also the SWNTs

themselves, although SWNTs tend to damage less easily. Hence, there is a very practical need for the careful design and evaluation of these oxidative treatments, as one needs to balance the requirements of impurity removal with that of conservation of SWNT structure and yield to ensure further nanotube processability in applications.

2.1.1. Liquid phase oxidative methods. Use of nitric acid (HNO_3) is common as it is straightforward, inexpensive, and fairly effective in removing metal catalysts and amorphous carbon from large quantities of raw material. Nitric acid can also introduce oxygenated groups at the ends of SWNTs. It is known for instance that refluxing or sonicating nitric acid opens SWNT ends and introduces carboxylic acid groups at these opened ends and defect sites on the sidewalls. In our group, we have used nitric acid purification for subsequent derivatization of SWNTs with crown ethers as well as with lanthanides in separate experiments.[41,45]

Sensitivity of SWNT materials to mildly oxidizing nitric acid treatment has been previously investigated by TEM.[48] Electron microscopy results show that acid purification can alter the structure of both SWNTs prepared by pulse laser vaporization (PLV) and arc-discharge methods (Fig. 4). It has been recently claimed based on solution-phase near-IR work that an HNO_3 oxidative purification method will inevitably destroy arc-discharge SWNTs, producing amorphous carbon to some extent.[28] That may not be surprising considering that even dimethylformamide (DMF), often used as a solvent, may attack and hence alter structural defect sites of SWNTs.[48] In the following sections, we describe the structural and purification-associated effects of oxidative treatments, such as nitric acid, on different types of carbon nanotubes.

2.1.1. (a). Liquid phase oxidation on nanotubes produced by laser ablation techniques. As-prepared SWNTs by laser ablation techniques, including pulsed laser vaporization (PLV), have relatively long bundles of tubes with few defects, and can be purified using a nitric acid treatment.[30,31,34,48–52] In a typical run,[49,50] raw tubes are refluxed in 2.6 M HNO_3 for 45 h. Upon cooling to room temperature, the mixture is then centrifuged, leaving a black precipitate and a clear, brownish yellow supernatant acid. The supernatant is then decanted and washed with deionized water multiple times prior to centrifugation; these steps may be repeated three more times for a 10 g batch of raw tubes. After washing, the mixture is resuspended in pH 10 water with surfactant, and ultimately filtered using a cross-flow filtration system.

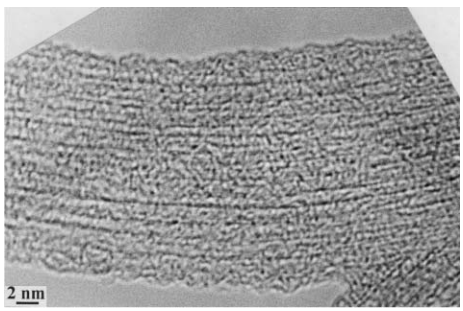

Fig. 4 Example of altered SWNT ropes from a mild-strength acid-treated material, produced from PLV. Short and distorted SWNT walls are associated with amorphous-like material. Reprinted with permission from ref. 48, M. Monthioux, B. W. Smith, B. Burteaux, A. Claye, J. E. Fischer, D. E. Luzzi, *Carbon*, 2001, **39**, 1251. Copyright (2004) Elsevier.

To obtain tubes of smaller lengths, sonication for 20 min in a 3 : 1 H_2SO_4–HNO_3 mixture is often employed. After filtration over a 0.2 μm polycarbonate membrane, the residue is then re-sonicated in distilled water for 30 min, and ultimately recovered upon filtration, after repeated washing. 'Polishing' of the tubes is accomplished by stirring the sample in a 4 : 1 mixture of H_2SO_4–30% H_2O_2(aq.) for 30 min. After dilution, filtration and washing, the tubes are washed with 35% HCl solution to ensure that carboxylic acid groups are formed at the ends and defect sites. Although this process involves a large number of steps with yields of ~10–20 wt.%, it has the advantage of batch scalability.[53,54] We and other groups have employed modifications of this protocol with different reaction times, temperatures, and acid concentrations, with similar results.

Dujardin *et al.* have reported a relatively simple, one-step method.[34] Briefly, raw materials were sonicated in concentrated nitric acid (70%) followed by refluxing at 120–130 °C for 4 h. The yield reached 50% of the sample, which appeared to reflect the initial nanotube content. The amount of metal decreased to as low as ~1%, as determined by chemical analysis. It was claimed that SWNTs were relatively inert toward the acid oxidation process, at least in their bundle form.

Typical nitric acid treatments have also been used in combination with other oxidative methodologies, such as air oxidation, to facilitate removal, in particular, of amorphous carbon. This approach is based on the fact that the etching rate of amorphous carbon is faster than that of carbon nanotubes. Further details are described in a subsequent section. Annealing at high temperature (873–1873 K) tends to consume defect sites[31,32,55,56] and to pyrolyze graphitic carbon and short fullerenes. Using a high temperature vacuum treatment (1873 K), annealing will melt and hence, remove metal.[57]

Dillon *et al.* have reported results of a non-destructive, scalable, three-step purification process that yields materials with >98 wt% purity.[30] Briefly, a dilute nitric acid (3 M HNO_3) reflux for 16 h digests, functionalizes, and redistributes the non-nanotube fractions so as to form a uniform and reactive coating on the SWNTs. This coating is selectively removed by oxidation in stagnant air. In addition, they investigated the effect of this procedure on arc-discharge SWNTs, and found that a relatively long period exposure consumed a significant fraction of the nanotubes themselves, due to the presence of a larger metal content.

Chiang *et al.* have employed similar acid purification procedures in purifying SWNTs but with the additional use of lower gas phase oxidation temperatures: first at 300 °C, then at 500 °C, with each step followed by HCl extraction washing.[31] They found that gas phase oxidation (5% O_2–Ar, 1 atm, 1 h) at temperatures greater than 500 °C yielded tubes with substantially less metal content. However, this procedure also resulted in a large loss of SWNTs. The quality of SWNT

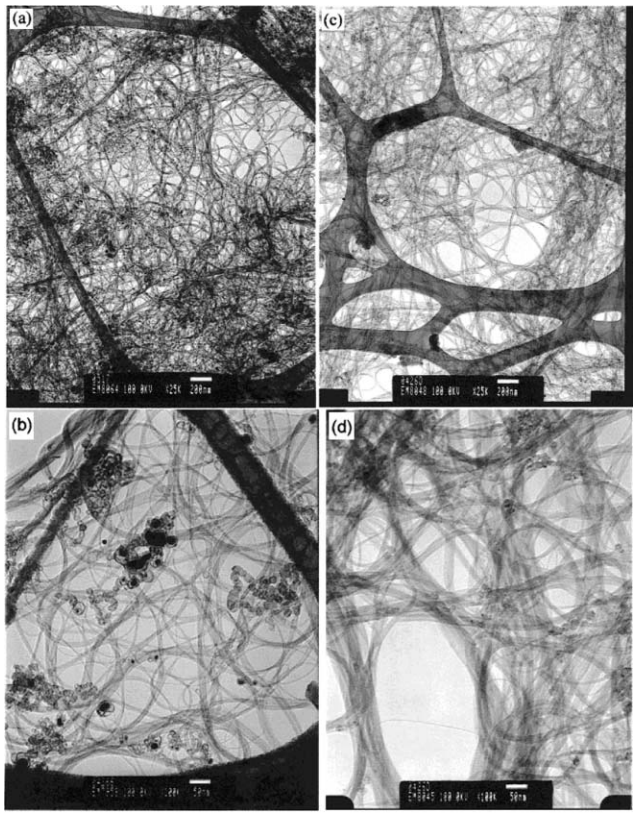

Fig. 5 TEM images of SWNTs. Before purification (as-purified Tubes@Rice SWNTs): (a) magnification = 25 000, (b) magnification = 100 000. After a two-stage purification process: (c) magnification = 25 000, (d) magnification = 100 000. Reprinted with permission from ref. 31, I. W. Chiang, B. E. Brinson, R. E. Smalley, J. L. Margrave, R. H. Hauge, *J. Phys. Chem. B*, 2001, **105**, 1157. Copyright (2001) American Chemical Society.

samples before and after the purification processes are shown in Fig. 5. Metal particles have been identified as dark particles (Fig. 5a and 5b), gathered into groups and associated with amorphous carbon. In the cleaned sample, most of the metal has been removed. However, some of amorphous carbon is still present (Fig. 5c and 5d).

Complete elimination of metal catalysts, even after extensive refluxing in nitric acid, was only observed after a sonication-mediated treatment in a 1 : 1 mixture of HF–HNO_3.[52] It has been suggested that the effectiveness of this methodology in removing metal catalysts arises from the relatively small size of HF and hence, its ability to better wet and react with these SWNTs.

2.1.1. (b). Liquid phase oxidation on nanotubes produced by arc-discharge technique. SWNT materials grown from arc-discharge synthetic process have also been purified using similar methods used in the purification of laser ablation growth SWNTs.[27,28,54,57–61] Arc discharge tubes are more impure, especially in terms of large metal content, but an initial first run at purification can be successful using a treatment involving either 3 M HNO_3 for 12 h or 7 M HNO_3 for 6 h.[28] Variations on this theme have been numerous.

For instance, refluxing in nitric acid has been followed by successive filtration steps (cross flow filtration (CFF) system).[59] The effects of each step were analyzed by SEM and TEM. After filtration, it was noted that metal catalysts were almost completely removed, leaving behind empty nanocapsules. Nanotube bundles were only slightly damaged with the resulting purity estimated to be higher than 90%.

Raw arc discharge SWNT bundles (Carbolex: length range of 0.8 to 1.2 μm; ~35–50 nm in width) were initially oxidized using $KMnO_4$. To summarize, nanotubes were sonicated and then refluxed in a boiling solution of $KMnO_4$ in sulfuric acid. Upon filtration, the tubes were washed extensively with HCl to dissolve away all of the MnO_2 and further washed multiple times with distilled, deionized water. This method is expected to functionalize and derivatize the nanotube sidewalls with keto, carboxylic, aldehyde, and alcoholic groups. In our group, we have used this permanganate oxidation in sulfuric acid coupled with HCl treatment to process tubes that were subsequently functionalized in separate experiments with Vaska's complex and with Wilkinson's complex. In other independent experiments, TiO_2 as well as CdSe nanocrystals were attached to nanotubes, processed as described, using a solution-phase technique.[39,40,42]

A three-step oxidation process for obtaining high-quality SWNTs from arc-discharge prepared soot has also been reported.[57] Mild oxidation (2.8 N HNO_3 reflux) was initially performed to form an oxide layer on the surface of metal to minimize the amount of oxidized or digested SWNTs in further steps. The sample was then heated in air at 550 °C for 10 min (air oxidation) to remove amorphous carbon, followed by a high-temperature vacuum annealing treatment (1600 °C at 10^{-3} Pa for 3 h) to decompose the resulting oxide layer, to remove remaining graphitic carbon and metals, and to permit extraction of SWNT materials with a yield of ~20 wt.% with less than 1% metal content.

In addition, a hydrothermal treatment (more specifically, a hydrothermally initiated dynamic extraction method, HIDE) has been employed,[54,58] wherein as-prepared SWNTs were sonicated in water and then refluxed with subsequent removal of fullerenes and other soluble components using toluene extraction. Washing was then performed using 6 M HCl, after heating and removal of amorphous carbon in air at 743 K. It was proposed that intervening H_2O molecules destroy the network between SWNTs and amorphous carbon as well as that involving metal particles, and even attack the graphitic layer encapsulating the metal particles. The purity reported was 95 wt% though unfortunately, the overall yield was less than 1%.

2.1.1. (c). Liquid phase oxidation used to purify chemical vapor deposition tubes. Oxidative treatments for these tubes tend to involve a variety of oxidants including 2.6 M nitric acid, a 3 : 1 98% H_2SO_4–HNO_3 (16 M) mixture, and $KMnO_4$.[62] Using FT-IR spectroscopy and TEM, dilute nitric acid was found to be a mild oxidant, which introduced carboxylic acid groups specifically at those sites which had already contained defects prior to this acid treatment. As a comparison, the use of $KMnO_4$ in alkali solution was found to be relatively mild. Varying amounts of –OH, –C=O, and

–COOH groups were introduced. In contrast, sonication of SWNTs in a H_2SO_4–HNO_3 mixture increased the incidence of carboxylic acid groups not only at initial defect sites but also at the newly created defect sites along the sidewalls of SWNTs. Moreover, this treatment substantially enriched the proportion of large-diameter SWNTs from ~3% to ~20% after 96 h of acid treatment[63].

2.1.2. Gas phase oxidation used to purify SWNTs. Gas phase oxidation (*i.e.*, heating in air, oxygen, or other gases) is based on the principle of a selective oxidative etching process, wherein the carbonaceous species are oxidized at a faster rate than the actual SWNTs themselves. After destruction of carbonaceous species such as amorphous carbon and graphitic carbon layers, the metal catalysts can be removed using acid treatment such as HCl washing. However, slightly different conditions necessarily need to be applied for SWNT materials grown from distinct synthetic methods, since the various classes of SWNTs will behave differently towards identical oxidative etching processes. A discussion of these various strategies ensues.

Zimmerman *et al.* reported a gas phase purification method incorporating Cl_2, H_2O, and HCl gaseous mixtures.[64] SWNTs grown from pulsed laser vaporization (PLV) were heated at 500 °C in the presence of the gaseous mixtures to remove carbonaceous species. After HCl treatment to dissolve away the metal impurities, the SWNT materials were subsequently filtered, yielding reasonably pure product. Arc-discharge grown SWNTs could not be purified by identical procedures, likely due to the differential densities of these two systems.

Nagasawa *et al.* have coupled gas phase oxidation by heat treatment in O_2 gas with nitric acid oxidation for SWNT materials grown by PLV.[65] It was found that SWNTs, with diameters in the range of 1.13 and 1.22 nm, burn more quickly than the 1.37 nm diameter tubes when heating in oxygen. Selective oxidation of thinner SWNTs was also observed upon refluxing in nitric acid.

To purify SWNTs grown from the arc-discharge method, gas phase oxidation in air in combination with a microfiltration method has been utilized. The burning temperature of SWNTs in air was 350 °C.[66] A high-yield purification process of arc-discharge grown SWNTs was achieved by combining thermal annealing in air with subsequent acid treatment.[60a] Gas phase oxidation was employed to eliminate carbonaceous species prior to acid washing. Briefly, the raw materials, which were mixed from several batches, were oxidized in air (at 470 °C) to burn out carbonaceous species, and were subsequently immersed and filtered in 6 M HCl to dissolve the metal catalysts. Furthermore, the samples were refluxed in nitric acid to unbundle SWNTs. The process was monitored by SEM and TEM. In the TEM data reported, nitric acid refluxing resulted in the formation of broken SWNT fragments and even MWNTs. The yield of tubes was very poor at temperatures greater than 500 °C. Use of long annealing times was found to be strongly dependent on the presence and identity of the metal catalysts in the samples, confirming that control of annealing temperature and times were of crucial importance in ensuring the high overall yield of SWNT materials. The optimized yield reported was 25–30 wt% with a purity level of ~96%, containing 1% metal particles from an initial value of 8%.

Arc-derived tubes have also been purified through a dry oxidation technique that initially removes amorphous carbon, followed by subsequent refluxing in two different acids (HCl and HNO_3) to remove Ni–Y metal.[60b] Individual purification steps were carefully studied using TGA, Raman scattering, AFM, and electron microscopy to show the effects of chemical processing. In addition, debundling and dissolution of the tubes were carried out using ultrasonic dispersion to generate isolated tubes in amide solvents, such as DMF or *n*-methyl-2-pyrrolidone (NMP). It was discovered that this treatment can yield as much as 90% isolated tubes, dispersed in amide solution; the damaged tube walls can be repaired by vacuum annealing at 1100 °C.

A systematic study, *i.e.* a quantitative estimation, of the effect of the purification of arc-discharge grown SWNT films by heating in flowing oxygen gas has also been reported.[26] Purity levels and amounts of SWNTs and carbonaceous impurities were monitored as a function of oxidation temperature and time. For example, at 315 °C, the etching rate of SWNTs was lower than that for amorphous carbon for the first 2 h. After 2 h oxidation, most of the amorphous carbon was etched away; further annealing only led to the actual destruction of SWNTs.

Recently, a method for the purification of SWNTs grown from most known synthetic processes such as arc-discharge, laser ablation, and HiPco was reported.[67] This method involves air oxidation, and acid washing followed by hydrogen treatment. After air oxidation at 300 °C, arc-discharge grown SWNTs were washed in nitric acid followed by hydrogen treatment at 1000 °C. Similar procedures were applied for laser ablation and HiPco SWNTs. After a CS_2 extraction, samples were dissolved in 8 N HCl solution. Amorphous carbon was still observed in the TEM data reported. Regarding the actual hydrogen treatment, HiPco SWNTs were heated at 700 °C, whereas arc-discharge and laser ablation tubes were heated to 1000 °C.

2.1.3 Various oxidative methods used to purify high-pressure carbon monoxide decomposition (HiPco) tubes. HiPco nanotubes,[68] which are produced by the high pressure decomposition of CO, have diameters in the range of 0.7–1.1 nm. These are thus smaller and more reactive on average than the tubes previously discussed. Conventional treatments with nitric acid mentioned above typically destroy HiPco SWNTs. Thus, these tubes require different purification protocols. Furthermore, the methods alluded to earlier are usually associated with very low tube yields and in eliminating the impurities, a substantial proportion of nanotubes are lost. The rationale for this problem is that while an exploitable differential reactivity exists between nanotubes and other forms of carbon, this difference is not very pronounced.

HiPco nanotubes,[68] however, are more than 90% pure, and contain very little amorphous carbon. This is due to the fact CO does not decompose easily at the temperatures required for the Boudouard reaction, the basis of HiPco formation. In fact, the major impurity of HiPco samples is iron, some of which is encapsulated by graphitic spheres. Fig. 1 shows an Fe particle

encapsulated by graphite layers. The challenge in purifying HiPco tubes thus is the ability to leach out metal from such relatively unreactive, protected sites without using aggressive oxidizing agents, so as not to destroy the tubes, while simultaneously obtaining a high yield after the purification process.

Wet air (or wet Ar–O_2) oxidation, at 180–300 °C, followed by HCl treatment, has been found to be quite effective at purifying HiPco nanotubes.[32] In wet air oxidation, Fe is oxidized to Fe_2O_3, which having a lower density, expands, cracking the graphitic shell. Thus, the Fe can now be attacked and leached by HCl, leaving behind onion-like shells of graphite. Wet air seems to be essential to the process, as H_2O is expected to help in the oxidation of Fe. Anhydrous oxygen, used as opposed to wet air, was less successful at removing iron.[24] In addition, oxygen was found to preferentially destroy smaller-diameter nanotubes. In our group, we have used wet air oxidation prior to the selective solution-phase sidewall osmylation of metallic SWNTs.[43, 69]

A mild H_2O_2 treatment can be used to destroy amorphous carbon and adsorbed organics without affecting the nanotube structure.[70d] Using a combination of solvent washing and repeated wet air oxidation steps, we can reduce the Fe content to fractions of 0.1% without destroying the tubes or affecting their electronic properties. Wet air oxidized nanotubes show very little amorphous contamination as shown in Fig. 6.

Very recently, iron catalyst particles and non-nanotube carbonaceous materials in raw HiPco have been removed through a multistep, scalable protocol.[70a] Specifically, carbon-coated iron nanoparticles are oxidized by O_2 and exposed in multistep oxidation steps at increasing temperatures (150–350 °C). Subsequently, the exposed metal oxide is deactivated by reaction with $C_2H_2F_4$ or SF_6 to its corresponding fluoride, which is subsequently removed by a Soxhlet extraction with a 6 M HCl solution.

A comparison between the effect of gas and liquid phase oxidation processes on HiPco nanotubes has been performed using absorption/Raman spectroscopy and TEM.[70b] It was found that whereas a liquid phase oxidative treatment, involving ultrasonication in a 3 : 1 acid mixture of H_2SO_4 to HNO_3, was found to continuously destroy narrow diameter SWNTs through the oxidation of the sidewalls of these materials, a gas phase oxidative treatment at high temperature could be used to preferentially oxidize SWNTs without introducing sidewall defects. Recently, this identical research group was able to effectively remove residual quantities of iron catalyst (of up to ~3%) from an aqueous surfactant solution of SWNTs by the application of a 1.3 T permanent magnet field.[70c] Absorbance spectra of the initial and resultant purified dispersions of SWNTs showed that the purification procedure did not dramatically affect the overall diameter distribution of these tubes.

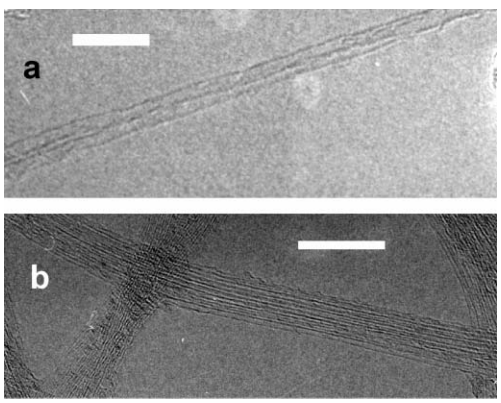

Fig. 6 HRTEM images of bundles of purified HiPco tubes showing cleaned surfaces bereft of amorphous carbon and metallic particle impurities. The scale bars indicate 5.5 nm and 17.5 nm, in parts (a) and (b) respectively.

2.2. SWNT purification methods based on chemical functionalization strategies

Purification of SWNTs can also be achieved as a byproduct of chemical functionalization protocols, many of which are focused on solubilizing SWNTs by introducing other functional groups onto tube surfaces rather than by pointedly removing impurities. The dissolution of SWNTs in organic solvents was initially achieved by the reaction of carboxylic acid functionalities at SWNT ends and defect sites with octadecylamine *via* the formation of an amide bond.[71] These soluble tubes allowed for the application of techniques such as GPC or HPLC as a means of tube purification.[72,73] To regain reasonable quantities of unfunctionalized but purified tubes, functional groups could be removed by thermal treatment.

2.2.1. Azomethine ylide. Georgakilas *et al.* have utilized SEM and TEM to monitor purification of SWNTs through organic functionalization using azomethine ylides.[74] It is believed that organic functionalization, as opposed to oxidation with oxidants, renders SWNTs easier to handle and hence, better for potential practical uses. As seen in the TEM image of the pristine (p-SWNTs), in Fig. 7a, a large quantity of metallic nanoparticles and amorphous carbon are present, which upon functionalization, largely disappear. Carbon impurities, mainly amorphous carbon, which had remained but which were soluble in DMF (f-SWNTs), in Fig. 7c, were slowly removed by slow precipitation of a solution of these tubes in chloroform utilizing diethyl ether. The last step of this purification process was the removal of functional groups and the recovery of purified nanotubes (r-SWNTs) by thermal treatment at 350 °C followed by annealing to 900 °C. A TEM image of the resulting product is seen in Fig. 7b; tubes are free of any impurities and demonstrate similar DSC characteristics to pristine SWNTs.

In general, while chemical functionalization is a credible alternative for purification of nanotubes, the number and complexity of steps involved sometimes can be disadvantageous. Moreover, intrinsic properties, such as the electronic properties of tubes, may also be altered.

2.2.2. Solution-phase ozonolysis. We have recently published work on the purification of HiPco SWNTs by solution phase ozonolysis.[38] This protocol is not only milder than other ozonolysis methods but also when combined with a cleavage

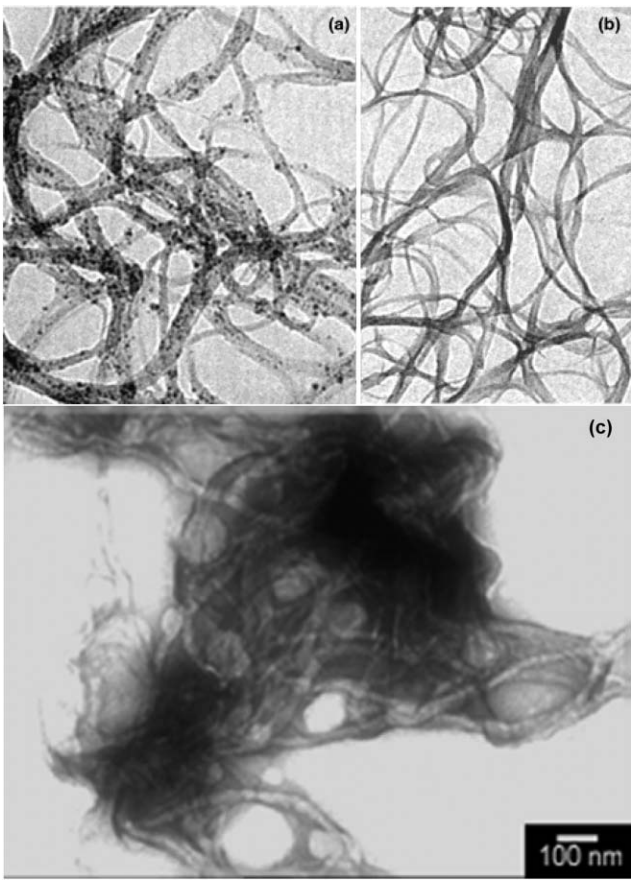

Fig. 7 Representative TEM images of (a) p-SWNT, (b) r-SWNT, and (c) f-SWNT prior to the purification step. Reprinted with permission from ref. 56, V. Georgakilas, D. Voulgaris, E. Vázquez, M. Prato, D. M. Guldi, A. Kukovecz, H. Kuzmany, *J. Am. Chem. Soc.*, 2002, **124**, 14318. Copyright (2002) American Chemical Society.

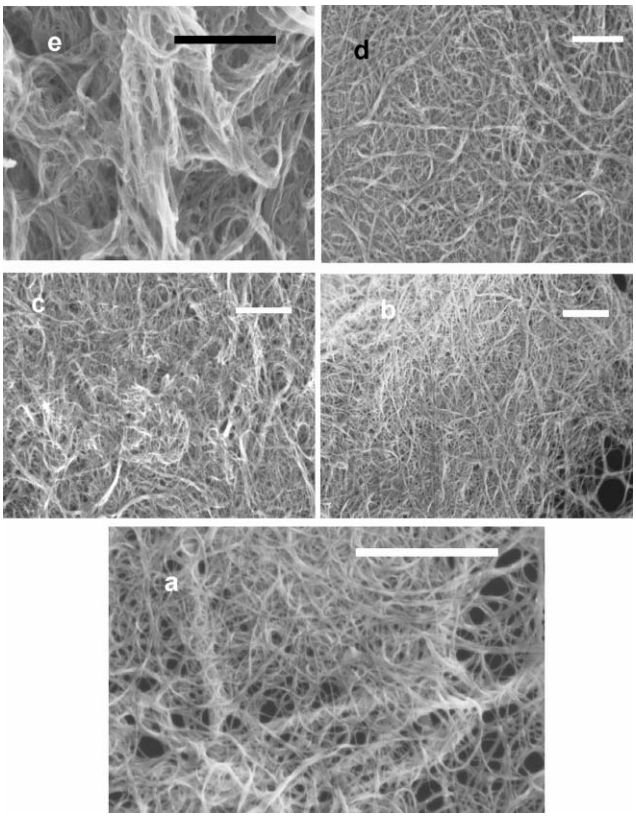

Fig. 8 Scanning electron micrographs of a number of SWNT samples: (a) ozonized sample **1** (with H_2O_2); (b) ozonized sample **2** (with DMS); (c) ozonized sample **3** (with $NaBH_4$); (d) Control ozonized sample; (e) raw, as-prepared HiPco. Scale bars for these micrographs are 1 μm in each case. Reprinted with permission from ref. 38, S. Banerjee, S. S. Wong, *J. Phys. Chem. B*, 2002, **106**, 12144. Copyright (2002) American Chemical Society.

reaction, increased purity of the nanotube can be achieved with minimal sample loss and controllable functional group composition. It is believed that O_3 adds to the double bonds of SWNTs through a facile 1,3-dipolar cycloaddition reaction following Criegee's mechanism, where the unstable ozonide formed may readily dissociate. We have recently found that ozonolysis is also selectively reactive for small-diameter tubes, rendering it possible to separate tubes on the basis of diameter.

In the context of purification, previous studies of ozonolysis of nanotubes in solution simply mention that the tubes have been opened and unfortunately, neither address purification nor the presence and location of functional groups. In our study, the SEM and TEM micrographs (Fig. 8) indicate the increased purity of the ozonized tubes, compared with as-prepared tubes. For instance, a large amount of contaminant material, particularly amorphous carbon in the initial, raw HiPco sample, is substantially removed after ozonolysis and associated treatments. This is not altogether surprising.

It is reasonable, for instance, to expect that upon ozonolysis, amorphous carbon detritus, onions, and nanoparticles will become heavily functionalized with oxygenated groups and thereby have increased solubility in polar solvents, used to wash these samples. The reactivity of these contaminant materials is analogous to the reactivity at the end caps of the tubes, which are opened upon oxidation.[26,30,31] Indeed, there is also enhanced reactivity in regions of increased curvature and conformational strain, notably at high densities of pentagonal and heptagonal defect sites.[31,32] Ozone can oxidize[10,13] the graphitic coating surrounding the Fe metal catalyst particles to their corresponding iron oxides, which can then breach the carbon shells, exposing metal particulates. As such, the ozonolysis process essentially facilitates the removal of the unwanted Fe metal by subsequent stirring and sonication, associated with the chemical processing of SWNTs during sidewall functionalization. During this procedure, the iron and iron oxide clusters from the SWNTs readily loosen. The smaller clusters are expected either to pass directly through the membrane or to transform into heavily oxidized carbon nanospheres, which are soluble in, or at least more easily dispersed in, polar solvents. Moreover, these clusters can be readily dissolved and hence removed by acid treatment. Use of acetic acid as a solvent is also rather effective at Fe removal.

We have demonstrated that hydrogen peroxide can leach iron oxide clusters into solution.[33] Thus, the O_3–H_2O_2 combined protocol should be very successful at removing iron, which is evident as seen in sample **1**, shown in Fig. 8a, to

a percentage of about 0.25% from a high of about 4–5% in unprocessed HiPco. Use of hydrogen peroxide alone, without ozonolysis treatment, is able to reduce the iron content to 1.37%, indicating the ability of this reagent to leach iron oxide clusters into solution. After ozonolysis, the processing of sample **3** involves an acid treatment to quench the borohydride reagent, which has the complementary effect of lowering Fe concentrations to only 0.48%. It is of note that a $NaBH_4$–HCl treatment, without ozonolysis, on the SWNTs can reduce the iron content in the sample to $\sim$1.16% only. The implication then is that most of the residual, extraneous iron is likely encapsulated within a carbon shell that needs to be reacted with ozonolysis, in order for it to be properly eliminated by means of HCl. Thus, ozonolysis, coupled with further specific chemical processing, appears to be best suited for SWNT purification.

2.3. SWNT purification methods based on filtration and chromatography

Microfiltration is based on size or particle separation. It is a physical-based purification technique. No chemical, oxidative treatment is required. Thus, microfiltration-based treatments neither result in huge sample loss nor in damaged or chemically altered SWNTs after the purification. A disadvantage of these procedures is the number of successive filtration steps necessary to achieve satisfactory purity as well as the fact that these methods do not readily yield size-selected tubes.

Bandow *et al.* reported a procedure for one-step SWNT purification by microfiltration in an aqueous solution, in the presence of a cationic surfactant.[33] As-prepared SWNTs by PLV were separated from coexisting metal nanoparticles, carbon nanospheres (CNS), polyaromatic carbons, and fullerenes without any oxidation used. Briefly, as-prepared SWNTs were soaked in CS_2 in order to extract polyaromatic carbons and fullerenes. Insoluble CS_2 matter were then trapped in a filter, and sonicated in an aqueous solution of 0.1% cationic surfactant (benzalkonium chloride) in order to separate the CNS and metal nanoparticles from the SWNTs. Through microfiltration with an overpressure of N_2 gas, most of the CNS, C_{60}, and C_{70} as well as metal nanoparticles were removed. This process was repeated for three cycles and monitored by SEM and TEM (Fig. 9). Most of the carbonaceous species can be identified as nanoparticles and are more clearly visible in Fig. 9a. On the other hand, relatively few CNS are observed in an image of a purified SWNT fraction in Fig. 9b. This method is, however, dependent on the initial purity of as-prepared SWNT materials. For example, for arc-discharge SWNTs, microfiltration could be combined with pretreatment using centrifugation, since these tubes contain low SWNT content.[33,35]

For a scalable continuous filtration process where the materials are efficiently suspended and the filter surface does not become contaminated with deposited material, Shelimov *et al.* reported an ultrasonically assisted filtration procedure.[75] It was found that nanotubes in purified samples were shorter than in the original pristine SWNT samples grown from PLV, due to some sonication-induced cutting of the nanotubes. Further refinements in the choice of surfactant and an increase in the number of filtration cycles may perhaps be crucial at improving separation.

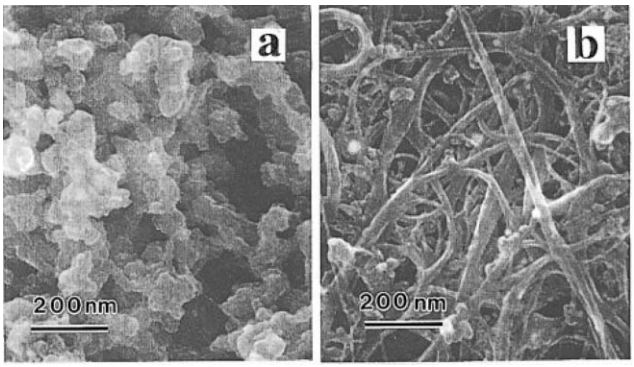

Fig. 9 Panels a and b represent the scanning electron micrographs taken for carbon nanoparticles (CNS) and SWNT fractions, respectively. Reprinted with permission from ref. 33, S. Bandow, A. M. Rao, K. A. Williams, A. Thess, R. E. Smalley, P. C. Eklund, *J. Phys. Chem. B*, 1997, **101**, 8839. Copyright (1997) American Chemical Society.

Chromatography, another non-destructive purification method, has been mainly used to separate small quantities of SWNTs into fractions with a small length and diameter distribution. Notably, gel permeation chromatography (GPC) and high performance liquid-phase chromatography coupled with size exclusion chromatography (HPLC-SEC) have been employed for this purpose.[72,73,76–80] Typical columns used for these procedures include a controlled-pore glass (CPG),[76,77,80] potassium polyacrylate,[78] Styragel HMW7,[72,73] and PLgel MIXED-A[79] materials, which have a number of pores of specific sizes, through which SWNT materials will flow through. This suggests that the smaller the molecule, the longer the pathway to the end of the column will be through a random walk. Hence, larger molecules will come off first. The pore size controls the nature of the size distribution that can be separated, so it has been possible to isolate highly purified SWNTs of specific length and diameter distributions without destroying or altering their intrinsic structures. However, since SWNT materials have to be either dispersed or solvated to be properly purified, chromatography is often used on a laboratory scale in conjunction with ultrasonification,[80] cross flow filtration (CFF),[80] or chemical functionalization.[72,73,79]

The collection of height images in AFM has often been used to estimate the effectiveness of the processes as well as size distributions of SWNT materials purified using column chromatography. Representative images are shown in Fig. 10.[78] Fig. 10a shows dispersed SWNT samples after nitric acid and ultrasonic treatments. This protocol fragments nanoparticles, while simultaneously destroying bundles. Fig. 10b shows a representative AFM image of the first fraction collected. Highly purified SWNTs can be clearly seen.

Functionalized or soluble SWNT materials also can be purified by chromatographic techniques.[72,73,79] For example, length separation of zwitterion-functionalized SWNTs has been performed using GPC, with the results shown in Fig. 11.[73] Fig. 11a shows the size-fractionation pattern of carboxyl-terminated, shortened (250 to 25 nm) SWNTs (sSWNT),

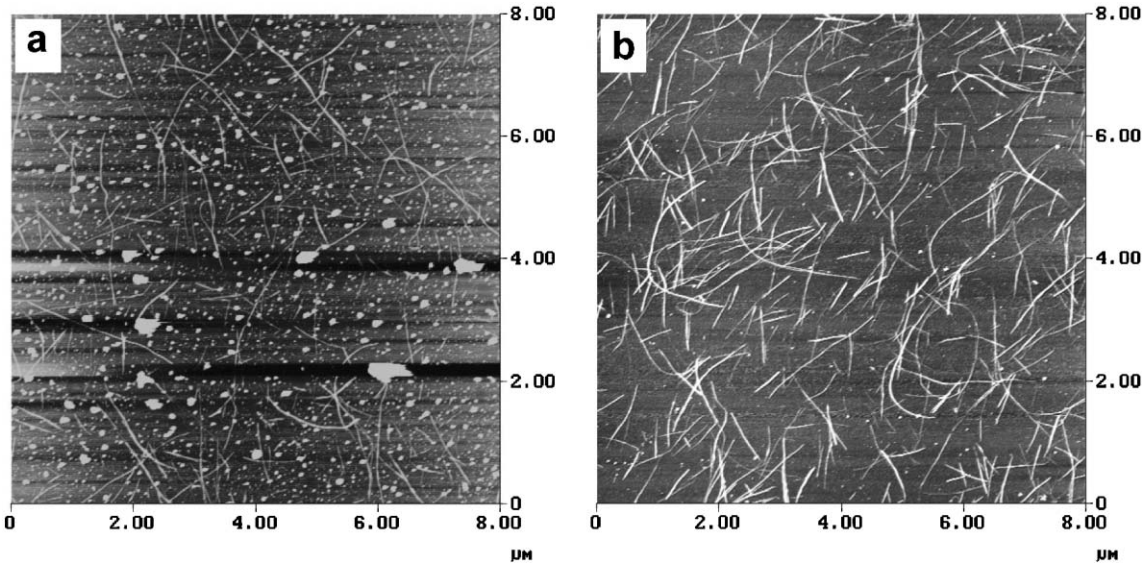

Fig. 10 (a) AFM image of SWNTs after nitric acid and ultrasonic treatment. This image clearly shows a large amount of impurities and single SWNT bundles. (b) AFM image of the first fraction. It shows a large number of SWNT bundles and only a very small amount of impurities (single dots). These impurities mostly consist of amorphous carbon, but there is also the possibility of catalyst particles still existing. Reprinted with permission from ref. 78, M. Holzinger, A. Hirsch, P. Bernier, G. S. Duesberg, M. Burghard, *Appl. Phys. A*, 2000, **70**, 599. Copyright (2000) Springer.

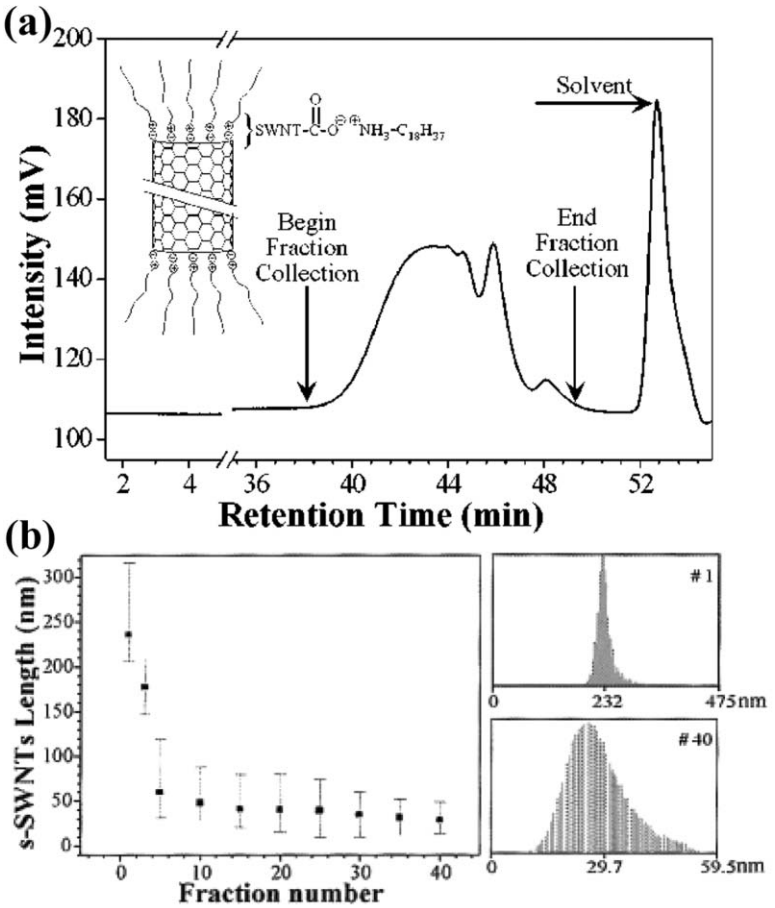

Fig. 11 (a) The chromatogram of sSWNTs/zwitterions in THF (Waters 600–996, styragel HMW7 column, refractrometer detector). (b) Distribution of sSWNTs lengths after fractionation, as monitored by AFM. The solid squares indicate weight-average length of nanotubes in each fraction whereas the error bars manifest the length distribution within 98% accuracy. The AFM-generated length histograms for fractions 1 and 40 are also illustrated. Reprinted with permission from ref. 73, D. Chattopadhyay, S. Lastella, S. Kim, F. Papadimitrakopoulos, *J. Am. Chem. Soc.*, 2002, **124**, 728. Copyright (2002) American Chemical Society.

whereas Fig. 11b depicts the weight-averaged length and distribution of tubes collected as a function of fraction number. Typical AFM-generated histograms demonstrate a relatively narrow length distribution within each fraction. Moreover, it is claimed that isolation and characterization of such fractions permit direct observation of all optically allowed transitions for both *met*- and *sem*-SWNTs, which could provide a sorting mechanism of single SWNTs by means of diameter as well as possibly by chirality.

2.4. SWNT purification methods based on microwave heating

Recently, the purification of arc-discharge SWNTs was accomplished using microwave heating in air.[81] The microwaves couple to the residual metal catalyst, significantly raising the local temperature, leading to both oxidation and rupturing of the carbon layer surrounding the catalyst particles. After microwave heating, as in ozonolysis, a mild acid digestion (4 M HCl) for 1–2 h was sufficient to remove most of metal catalysts (>0.2 wt.%).

After a short microwave treatment of SWNTs at 500 °C for 20 min in flowing dry air, the carbon coating was observed to be almost completely removed from the surfaces of most of the metal catalysts. The local temperature at the particle surface is likely to be caused by some sintering of the metal particles. HRTEM images of SWNT ropes taken after refluxing in 4 M HCl acid for 6 h showed that the ropes remained relatively intact with most of the metal particles removed by the HCl treatment. Microwave treatment also drastically reduced processing times to ~1 h, as compared with conventional acid reflux methods (45 h).[82]

Overall, microwave heating should be more effective at purifying arc-discharge SWNTs as opposed to laser ablation SWNTs because of the higher metal content of arc-discharge SWNTs. Furthermore, as compared with many of the selective oxidation methods described above, this protocol did not damage the SWNTs as much. In addition, processing time for purification was relatively short as compared with traditional refluxing techniques.

3. Conclusions

Purification of SWNT materials depends on the removal of impurities such as metallic and carbonaceous impurities, while leaving the structure of the actual SWNTs intact. The purification techniques that have been discussed in the previous sections indicate that care should be taken as to which particular technique is chosen, as different techniques often lead to different results. An algorithm for the rational purification of SWNTs shown in Fig. 3 can be commonly and readily evaluated using microscopy techniques, including TEM, SEM, and AFM. Microscopy is thus seen to be useful at every step in the purification protocol: namely, to identify impurities and to simultaneously monitor tube structure and purity.

Several other methods have not been discussed, including annealing which has the ability to modify the nanotube structure and consume functional groups at defect sites;[31,32,55–57] sonication which allows for the separation and dispersion of SWNTs as well as the oxidation of carbonaceous species in acid;[31–34,52,63,75,80] the mediation of ultrafine nanoparticles;[83–85] cutting using fluorination;[86] polymer-mediated ultrasonication;[87] and lithium intercalation.[88] The ultimate goal of all of these protocols is the purification of a large quantity of the SWNTs as well as their isolation and separation according to their length, diameter, and even chirality. The availability of such purified SWNTs will allow for fulfillment of their potentially fascinating applications as well as the understanding of their fundamental properties.

Acknowledgements

We acknowledge support of this work through startup funds provided by the State University of New York at Stony Brook as well as Brookhaven National Laboratory. Acknowledgment is also made to the US Department of Energy Office of Basic Energy Sciences (under contract DE-AC02-98CH10886) for facility use, the National Science Foundation for a CAREER award (DMR-0348239) and to the donors of the Petroleum Research Fund, administered by the American Chemical Society, for support of this research. SSW thanks 3M for a non-tenured faculty award. We also thank Dr J. Quinn (Stony Brook) and Dr J. Huang (Boston College) for SEM/TEM work and HRTEM analysis, respectively, for assistance with our microscopy analysis.

References

1 S. Iijima and T. Ichihashi, *Nature*, 1993, **363**, 603.
2 M. S. Dresselhaus, G. Dresselhaus and P. Avouris, *Carbon Nanotubes: Synthesis, Structure, Properties, and Applications*, Springer-Verlag, Berlin, 2001.
3 J. M. Planeix, N. Coustel, B. Coq, V. Brotons, P. S. Kumbhar, R. Dutartre, P. Bernier and P. M. Ajayan, *J. Am. Chem. Soc.*, 1994, **116**, 7935.
4 P. Calvert, *Nature*, 1999, **399**, 210.
5 J. Kong, N. R. Franklin, C. Zhou, M. G. Chapline, S. Peng, K. Cho and H. Dai, *Science*, 2000, **287**, 622.
6 P. G. Collins, K. Bradley, M. Ishigami and A. Zettl, *Science*, 2000, **287**, 1801.
7 R. H. Baughman, C. Cui, A. A. Zakhidov, Z. Iqbal, J. N. Barisci, G. M. Spinks, G. G. Wallace, A. Mazzoldi, D. D. Rossi, A. G. Rinzler, O. Jaschinski, S. Roth and M. Kertesz, *Science*, 1999, **284**, 1340.
8 A. C. Dillon, K. M. Jones, T. A. Bekkedahl, C. H. Kiang, D. S. Bethune and M. J. Heben, *Nature*, 1997, **386**, 377.
9 C. Liu, Y. Y. Fan, M. Liu, H. T. Cong, H. M. Cheng and M. S. Deresselhaus, *Science*, 1999, **286**, 1127.
10 C.-M. Yang, H. Kanoh, K. Kaneko, M. Yudasaka and S. Iijima, *J. Phys. Chem. B*, 2002, **106**, 8994.
11 W. A. de Heer, A. Châtelain and D. Ugarte, *Science*, 1995, **270**, 1179.
12 S. Fan, M. G. Chapline, N. R. Franklin, T. W. Tombler, A. M. Cassell and H. Dai, *Science*, 1999, **283**, 512.
13 S. S. Wong, E. Joselevich, A. T. Woolley, C. L. Cheung and C. M. Lieber, *Nature*, 1998, **394**, 52.
14 S. Saito, *Science*, 1997, **278**, 77.
15 M. Ouyang, J.-L. Huang and C. M. Lieber, *Acc. Chem. Res.*, 2002, **35**, 1018.
16 P. Avouris, *Acc. Chem. Res.*, 2002, **35**, 1026.
17 A. Bachtold, P. Hadley, T. Nakanishi and C. Dekker, *Science*, 2001, **294**, 1317.
18 B. C. Satishkumar, P. J. Thomas, A. Govindaraj and C. N. R. Rao, *Appl. Phys. Lett.*, 2000, **77**, 2530.
19 C. Journet, W. K. Maser, P. Bernier, A. Loiseau, M. Lamy de la Chapelle, L. S., P. Deneard, R. Lee and J. E. Fishcher, *Nature*, 1997, **388**, 1997.

20 A. Thess, R. Lee, P. Nikolaev, H. Dai, P. Petit, J. Robert, C. Xu, Y. H. Lee, S. G. Kim, A. G. Rinzler, D. T. Colbert, G. E. Scuseria, D. Tománek, J. E. Fischer and R. E. Smalley, *Science*, 1996, **273**, 483.
21 T. Guo, P. Nikolaev, A. Thess, D. T. Colbert and R. E. Smalley, *Chem. Phys. Lett.*, 1995, **243**, 49.
22 J. Kong, A. M. Cassell and H. Dai, *Chem. Phys. Lett.*, 1998, **292**, 567.
23 (*a*) S. Banerjee, T. Hemraj-Benny and S. S. Wong, *Adv. Mater.*, 2005, **17**, 17; (*b*) R. G. Ding, G. Q. Lu, Z. F. Yan and M. A. Wilson, *J. Nanosci. Nanotechnol.*, 2001, **1**, 7; (*c*) S. Banerjee, T. Hemraj-Benny and S. S. Wong, *J. Nanosci. Nanotechnol.*, 2005, **5**, 841.
24 W. Zhou, Y. H. Ooi, R. Russo, P. Papanek, D. E. Luzzi, J. E. Fischer, M. J. Bronikowski, P. A. Willis and R. E. Smalley, *Chem. Phys. Lett.*, 2001, **350**, 6.
25 M. S. Dresselhaus, G. Dresselhaus, A. Jorio, A. G. Souza Filho, M. A. Pimenta and R. Saito, *Acc. Chem. Res.*, 2002, **35**, 1070.
26 R. Sen, S. M. Rickard, M. E. Itkis and R. C. Haddon, *Chem. Mater.*, 2003, **15**, 4273.
27 M. E. Itkis, D. E. Perea, S. Niyogi, S. M. Rickard, M. A. Hamon, H. Hu, B. Zhao and R. C. Haddon, *Nano Lett.*, 2003, **3**, 309.
28 H. Hu, B. Zhao, M. E. Itkis and R. C. Haddon, *J. Phys. Chem. B*, 2003, **107**, 13838.
29 Y. Li, D. Mann, M. Rolandi, W. Kim, A. Ural, S. Hung, A. Javey, J. Cao, D. Wang, E. Yenilmez, Q. Wang, J. F. Gibbons, Y. Nishi and H. Dai, *Nano Lett.*, 2004, **4**, 317.
30 A. C. Dillon, T. Gennett, K. M. Jones, J. L. Alleman, P. A. Parilla and M. J. Heben, *Adv. Mater.*, 1999, **11**, 1354.
31 I. W. Chiang, B. E. Brinson, R. E. Smalley, J. L. Margrave and R. H. Hauge, *J. Phys. Chem. B*, 2001, **105**, 1157.
32 I. W. Chiang, B. E. Brinson, A. Y. Huang, P. A. Willis, M. J. Bronikowski, J. L. Margrave, R. E. Smalley and R. H. Hauge, *J. Phys. Chem. B*, 2001, **105**, 8297.
33 (*a*) S. Bandow, A. M. Rao, K. A. Williams, A. Thess, R. E. Smalley and P. C. Eklund, *J. Phys. Chem. B*, 1997, **101**, 8839; (*b*) Z. L. Wang, *Adv. Mater.*, 2003, **15**, 1497; (*c*) M. Yeadon, in *In-situ* Microscopy of Nanoparticles, *Encyclopedia of Nanoscience and Nanotechnology*, ed. H. S. Nalwa, American Scientific Publishers, Stevenson Ranch, CA, 2004, vol. **4**, p. 193.
34 E. Dujardin, T. W. Ebbesen, A. Krishnan and M. M. J. Treacy, *Adv. Mater.*, 1998, **10**, 611.
35 S. Bandow, S. Asaka, X. Zhao and Y. Ando, *Appl. Phys. A*, 1998, **67**, 23.
36 G. S. Duesberg, J. Muster, H. J. Byrne, S. Roth and B. M., *Appl. Phys. A*, 1999, **69**, 269.
37 S. Banerjee, M. G. C. Kahn and S. S. Wong, *Chem.—Eur. J.*, 2003, **9**, 1898.
38 (*a*) S. Banerjee and S. S. Wong, *J. Phys. Chem. B*, 2002, **106**, 12144; (*b*) S. Banerjee and S. S. Wong, *Nano Lett.*, 2004, **4**, 1445.
39 (*a*) S. Banerjee and S. S. Wong, *Nano Lett.*, 2002, **2**, 195; (*b*) S. Banerjee and S. S. Wong, *J. Am. Chem. Soc.*, 2003, **125**, 10342; (*c*) S. Banerjee and S. S. Wong, *Chem. Commun.*, 2004, 1866.
40 S. Banerjee and S. S. Wong, *J. Am. Chem. Soc.*, 2002, **124**, 8940.
41 M. G. C. Kahn, S. Banerjee and S. S. Wong, *Nano Lett.*, 2002, **2**, 1215.
42 S. Banerjee and S. S. Wong, *Nano Lett.*, 2002, **2**, 49.
43 S. Banerjee and S. S. Wong, *J. Am. Chem. Soc.*, 2004, **126**, 2073.
44 S. Banerjee and S. S. Wong, *Adv. Mater.*, 2004, **16**, 34.
45 T. Hemraj-Benny, S. Banerjee and S. S. Wong, *Chem. Mater.*, 2004, **16**, 1855.
46 S. S. Wong and S. Banerjee, in *Functionalization of Nanotube Surfaces*, ed. J. A. Schwarz, C. I. Contescu and K. Putyera, Marcel Dekker Inc, New York, 2004, pp 1251–1268.
47 S. Niyogi, M. A. Hamon, H. Hu, B. Zhao, P. Bhowmik, R. Sen, M. E. Itkis and R. C. Haddon, *Acc. Chem. Res.*, 2002, **35**, 1105.
48 M. Monthioux, B. W. Smith, B. Burteaux, A. Claye, J. E. Fischer and D. E. Luzzi, *Carbon*, 2001, **39**, 1251.
49 J. Liu, A. G. Rinzler, H. Dai, J. H. Hafner, R. K. Bradley, P. J. Boul, A. Lu, T. Iverson, K. Shelimov, C. B. Huffman, F. Rodriguez-Macias, Y.-S. Shon, T. R. Lee, D. T. Colbert and R. E. Smalley, *Science*, 1998, **280**, 1253.
50 A. G. Rinzler, J. Liu, H. Dai, P. Nikolaev, C. B. Huffman, F. J. Rodríguez-Macías, P. J. Boul, A. H. Lu, D. Heymann, D. T. Colbert, R. S. Lee, J. E. Fischer, A. M. Rao, P. C. Eklund and R. E. Smalley, *Appl. Phys. A*, 1998, **67**, 29.
51 C. Bower, A. Kleinhammes, Y. Wu and O. Zhou, *Chem. Phys. Lett.*, 1998, **288**, 481.
52 D. Chattopadhyay, I. Galeska and F. Papadimitrakopoulos, *Carbon*, 2002, **40**, 985.
53 T. W. Ebbesen, P. M. Ajayan, H. Hiura and K. Tanigaki, *Nature*, 1994, **367**, 519.
54 K. Tohji, T. Goto, H. Takahashi, Y. Shinoda, N. Shimizu, B. Jeyadevan, Y. Saito, A. Kasuya, T. Ohsuna, K. Hiraga and Y. Nishina, *Nature*, 1996, **383**, 679.
55 E. Borowiak-Palen, T. Pichler, X. Liu, M. Knupfer, A. Graff, O. Jost, W. Pompe, R. J. Kalenczuk and J. Fink, *Chem. Phys. Lett.*, 2002, **363**, 567.
56 V. Georgakilas, D. Voulgaris, E. Vázquez, M. Prato, D. M. Guldi, A. Kukovecz and H. Kuzmany, *J. Am. Chem. Soc.*, 2002, **124**, 14318.
57 H. Kajiura, S. Tsutsui, H. Huang and Y. Murakami, *Chem. Phys. Lett.*, 2002, **364**, 586.
58 K. Tohji, H. Takahashi, Y. Shinoda, N. Shimizu, B. Jeyadevan, I. Matsuoka, Y. Saito, A. Kasuya, S. Ito and Y. Nishina, *J. Phys. Chem. B*, 1997, **101**, 1974.
59 L. Vaccarini, C. Goze, R. Aznar, V. Micholet, C. Journet and P. Bernier, *Synth. Met.*, 1999, **103**, 2492.
60 (*a*) J.-M. Moon, K. H. An, Y. H. Lee, Y. S. Park, D. J. Bae and G.-S. Park, *J. Phys. Chem. B*, 2001, **105**, 5677; (*b*) C. A. Furtado, U. J. Kim, H. R. Gutierrez, L. Pan, E. C. Dickey and P. C. Eklund, *J. Am. Chem. Soc.*, 2004, **126**, 6095.
61 H. Huang, H. Kajiura, A. Yamada and M. Ata, *Chem. Phys. Lett.*, 2002, **356**, 567.
62 J. Zhang, H. Zou, Q. Qing, Y. Yang, Q. Li, Z. Liu, X. Guo and Z. Du, *J. Phys. Chem. B*, 2003, **107**, 3712.
63 Y. Yang, H. Zou, B. Wu, Q. Li, J. Zhang, Z. Liu, X. Guo and Z. Du, *J. Phys. Chem. B*, 2002, **106**, 7160.
64 J. L. Zimmerman, R. K. Bradley, C. B. Huffman, R. H. Hauge and J. L. Margrave, *Chem. Mater.*, 2000, **12**, 1361.
65 S. Nagasawa, M. Yudasaka, K. Hirahara, T. Ichihashi and S. Iijima, *Chem. Phys. Lett.*, 2000, **328**, 374.
66 Z. Shi, Y. Lian, F. Liao, X. Zhou, Z. Gu, Y. Zhang and S. Iijima, *Solid State Commun.*, 1999, **112**, 35.
67 S. R. C. Vivekchand, A. Govindaraj, M. Motin Seikh and C. N. R. Rao, *J. Phys. Chem. B*, 2004, **108**, 6935.
68 P. Nikolaev, M. J. Bronikowski, K. Bradley, F. Rohmund, D. T. Colbert, K. A. Smith and R. E. Smalley, *Chem. Phys. Lett.*, 1999, **313**, 91.
69 J. L. Bahr and J. M. Tour, *Chem. Mater.*, 2001, **13**, 3823.
70 (*a*) Y-Q. Xu, H. Peng, R. H. Hauge and R. E. Smalley, *Nano Lett.*, 2005, **5**, 163; (*b*) J. G. Wiltshire, A. N. Khlobystrov, L. J. Li, S. G. Lyapin, G. A. D. Briggs and R. J. Nicholas, *Chem. Phys. Lett.*, 2004, **386**, 239; (*c*) J. G. Wiltshire, L. J. Li, A. N. Khlobystrov, C. J. Padbury, G. A. D. Briggs and R. J. Nicholas, *Carbon*, 2005, **43**, 1151; (*d*) O. Zhou, H. Shimoda, B. Gao, S. Oh, L. Fleming and G. Yue, *Acc. Chem. Res.*, 2002, **35**, 1045.
71 J. Chen, M. A. Hamon, H. Hu, Y. Chen, A. M. Rao, P. C. Eklund and R. C. Haddon, *Science*, 1998, **282**, 95.
72 S. Niyogi, H. Hu, M. A. Hamon, P. Bhowmik, B. Zhao, S. M. Rozenzhak, J. Chen, M. E. Itkis, M. S. Meier and R. C. Haddon, *J. Am. Chem. Soc.*, 2001, **123**, 733.
73 D. Chattopadhyay, S. Lastella, S. Kim and F. Papadimitrakopoulos, *J. Am. Chem. Soc.*, 2002, **124**, 728.
74 V. Georgakilas, K. Kordatos, M. Prato, D. M. Guldi, M. Holzinger and A. Hirsch, *J. Am. Chem. Soc*, 2002, **124**, 760–761.
75 K. B. Shelimov, R. O. Esenaliev, A. G. Rinzler, C. B. Huffman and R. E. Smalley, *Chem. Phys. Lett.*, 1998, **282**, 429.
76 G. S. Duesberg, J. Muster, V. Krstic, M. Burghard and S. Roth, *Appl. Phys. A*, 1998, **67**, 117.
77 G. S. Duesberg, W. Blau, H. J. Byrne, J. Muster, M. Burghard and S. Roth, *Synth. Met.*, 1999, **103**, 2484.
78 M. Holzinger, A. Hirsch, P. Bernier, G. S. Duesberg and M. Burghard, *Appl. Phys. A*, 2000, **70**, 599.
79 B. Zhao, H. Hu, S. Niyogi, M. E. Itkis, M. A. Hamon, P. Bhowmik, M. S. Meier and R. C. Haddon, *J. Am. Chem. Soc.*, 2001, **123**, 11673.
80 E. Farkas, M. E. Anderson, Z. Chen and A. G. Rinzler, *Chem. Phys. Lett.*, 2002, **363**, 111.

81 A. R. Harutyunyan, B. K. Pradhan, J. Chang, G. Chen and P. C. Eklund, *J. Phys. Chem. B*, 2002, **106**, 8671.
82 M. T. Martínez, M. A. Callejas, A. M. Benito, W. K. Maser, M. Cochet, J. M. Andrés, J. Schreiber, O. Chauvet and J. L. G. Fierro, *Chem. Commun.*, 2002, 1000.
83 L. Thiên-Nga, K. Hernadi, E. Ljubovic, S. Garaj and L. Forró, *Nano Lett.*, 2002, **2**, 1349.
84 E. Mizoguti, F. Nihey, M. Yudasake, S. Iijima, T. Ichihashi and K. Nakamura, *Chem. Phys. Lett.*, 2000, **321**, 297.
85 M. Zhang, M. Yudasaka, F. Nihey and S. Iijima, *Chem. Phys. Lett.*, 2000, **328**, 350.
86 Z. Gu, H. Peng, R. H. Hauge, R. E. Smalley and J. L. Margrave, *Nano Lett.*, 2002, **2**, 1009.
87 M. Yudasaka, M. Zhang, C. Jabs and S. Iijima, *Appl. Phys. A*, 2000, **71**, 449.
88 B. Gao, C. Bower, J. D. Lorentzen, L. Fleming, A. Kleinhammes, X.-P. Tang, L. E. McNeil, Y. Wu and O. Zhou, *Chem. Phys. Lett.*, 2000, **327**, 69.

